Journal Pre-proofs

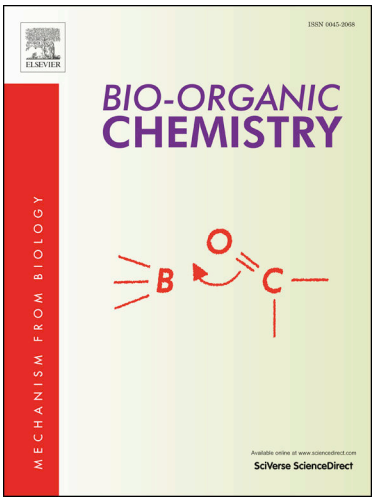

Development of Pyridazine Derivatives as Potential EGFR inhibitors and Apoptosis Inducers: Design, Synthesis, Anticancer Evaluation, and Molecular Modeling Studies

Marwa F. Ahmed, Eman Y. Santali, Eman M. Mohi El-Deen, Ibrahim A. Naguib, Radwan El-Haggar

PII: S0045-2068(20)31771-5
DOI: https://doi.org/10.1016/j.bioorg.2020.104473
Reference: YBIOO 104473

To appear in: *Bioorganic Chemistry*

Received Date: 12 October 2020
Revised Date: 10 November 2020
Accepted Date: 11 November 2020

Please cite this article as: M.F. Ahmed, E.Y. Santali, E.M. Mohi El-Deen, I.A. Naguib, R. El-Haggar, Development of Pyridazine Derivatives as Potential EGFR inhibitors and Apoptosis Inducers: Design, Synthesis, Anticancer Evaluation, and Molecular Modeling Studies, *Bioorganic Chemistry* (2020), doi: https://doi.org/10.1016/j.bioorg.2020.104473

Development of Pyridazine Derivatives as Potential EGFR inhibitors and Apoptosis Inducers: Design, Synthesis, Anticancer Evaluation, and Molecular Modeling Studies

Marwa F. Ahmed [1,2*]; Eman Y. Santali [1]; Eman M. Mohi El-Deen [3]; Ibrahim A. Naguib [1,4]; Radwan El-Haggar [2*]

[1] *Department of Pharmaceutical Chemistry, College of Pharmacy, Taif University, P.O. Box 11099, Taif 21944, Saudi Arabia.*

[2] *Department of Pharmaceutical Chemistry, Faculty of Pharmacy, Helwan University, Cairo, 11795, Egypt.*

[3] *Department of Therapeutic Chemistry, National Research Centre, Dokki, Cairo, 12622 Egypt.*

[4] *Pharmaceutical Analytical Chemistry Department, Faculty of Pharmacy, Beni-Suef University, Alshaheed Shehata Ahmad Hegazy St., 62514, Beni-Suef, Egypt*

Key words: Pyridazine, Pyrazoline; Antiproliferation; epidermal growth factor receptor, Apoptosis, Molecular docking.

*** Corresponding authors**:

Dr. Radwan El-Haggar, **Email:** radwan_elhaggar@pharm.helwan.edu.eg

Dr. Marwa F. Ahmed, **Email:** marwa.farg@tu.edu.sa

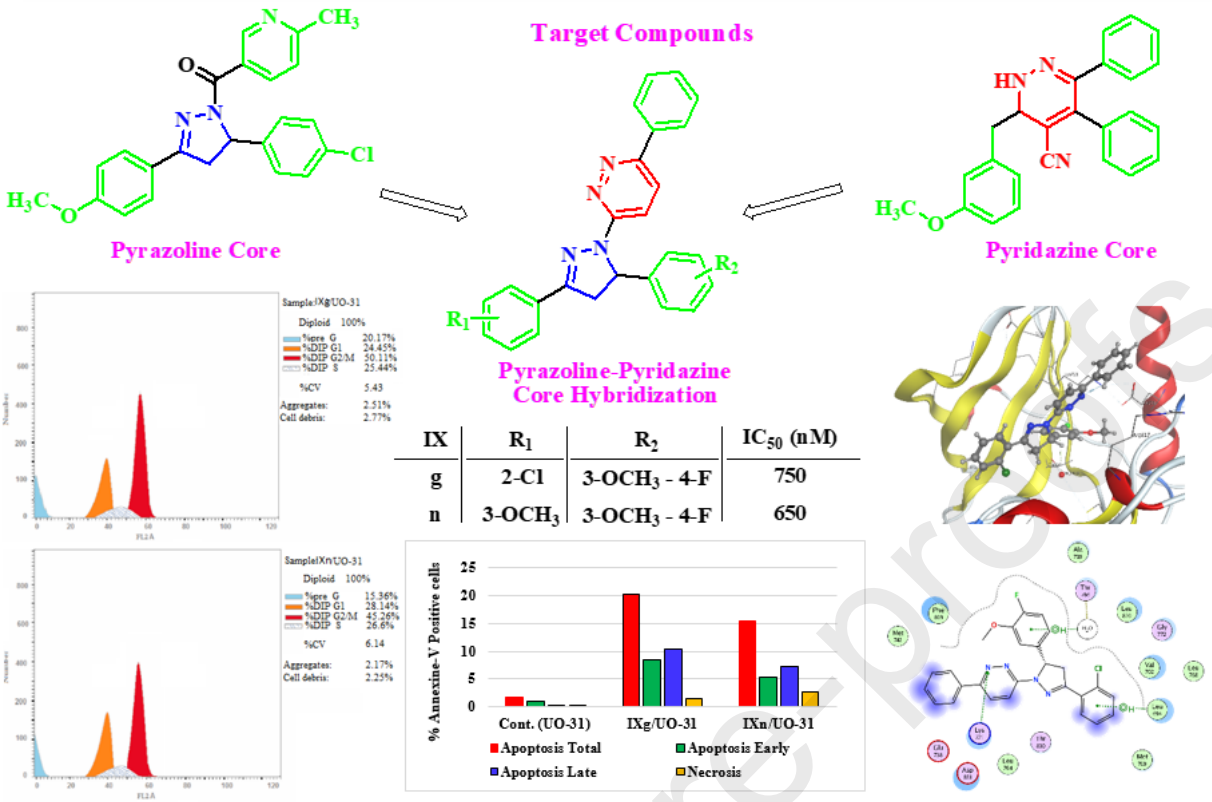

Highlights:

- Novel hybrids of pyridazine-pyrazoline were synthesized aiming to develop new antiproliferative candidates
- All compounds were submitted to the National Cancer Institute (NCI), USA, and many were proved to have significant antiproliferative activity.
- The enzyme inhibitory activity of compounds against epidermal growth factor receptor (EGFR) was evaluated
- A cell cycle analysis and an annexin V-FITC apoptosis assay of the most active compounds was tested.
- all synthesized compounds were subjected to molecular modeling studies using MOE software on the EGFR 3D structure and using Erlotinib as a reference compound.

Abstract

Novel hybrids of pyridazine-pyrazoline were synthesized aiming to develop new antiproliferative candidates. All compounds were submitted to the National Cancer Institute (NCI), USA, and many were proved to have significant antiproliferative activity. In addition, *in vitro* studies of the epidermal growth factor receptor (EGFR) inhibition showed that compounds **IXn**, **IXg**, **IXb** and **IXl** exhibited excellent inhibitory effect (IC_{50}=0.65, 0.75, 0.82 and 0.84 μM, respectively) compared to Erlotinib (IC_{50}=0.95 μM). The mechanistic effectiveness in cell cycle progression, apoptotic induction and gene regulation were assessed for the promising compounds **IXg** and **IXn** due to their significant EGFR inhibition. Flow cytometeric analysis indicated that compounds **IXg** and **IXn** result in increased cell numbers in phase G2/M, suggesting cell cycle arrest in phase G2/M in UO-31cells. Furthermore, real time PCR assay illustrated that compounds **IXg** and **IXn** elevated Bax/Bcl2 ratio which confirmed the mechanistic pathway of them. Moreover, the apoptotic induction of UO-31 renal cancer cells was enhanced effectively through activation of caspase-3 by compounds **IXg** and **IXn**. On the other hand, molecular docking study was performed to investigate binding mode of interaction of compounds with EGFR-PK in the active site with the aim of rationalizing its promising inhibitory activity. Finally, based on the aforementioned findings, compounds **IXg** and **IXn** could be considered as effective apoptosis modulators and promising leads for future development of new anti-renal cancer agents.

1. Introduction

Despite the rapid advance in drug discovery, the lack of effectiveness, safety and selectivity of anticancer drugs currently available remained as the most important unsolved issue [1]. Targeted therapy, a special type of chemotherapy, is a useful method

for preventing the growth and spread of cancer cells by targeting specific genes or proteins [2]. Advancing our knowledge of molecular and cellular biology enhances our ability to target specific cancer cell functions [3]. The human epidermal growth factor receptor (EGFR) is a tyrosine kinase (RTK) transmembrane receptor consisting of a single polypeptide chain of 1186 amino acids [4, 5]. This receptor belongs to the receptor family ErbB (human epidermal receptor, HER) which comprises four structurally related members EGFR (ErbB1), ErbB2 (HER2), ErbB3 (HER3) and ErbB4 (HER4) [6]. EGFR and members of its family play crucial roles in controlling many cellular processes including cell migration, survival, and proliferation [7]. EGFR may be triggered aberrantly by mutations or over-expression, leading to cell proliferation, angiogenesis, metastasis, and anti-apoptosis. EGFR is over-expressed in a variety of epidermal cancers including head and neck, chest, prostate, breast, cervical, brain and pancreatic cancers [8-10]. Considering that EGFR is a rational target for antitumor strategies, one of the most effective methods of inhibiting EGFR is blocking tyrosine kinase by small-molecule inhibitors at the ATP-binding site in the cytoplasmic domain [6].

In recent years, various nitrogen heterocyclic rings have remarkably complex biological properties and belong to one of the most important classes of medicinal chemistry compounds [11]. Pyrazole motif shows many applications in the field of pharmaceutical and medicinal chemistry. They have anti-inflammatory [12], fungistatic [13], analgesic [14], antibacterial [15], and potent antitumor activities [16-21]. A series of novel compounds containing the pyrazole motifs were reported as potent anticancer agents targeting EGFR tyrosine kinase [22-26]. Furthermore, pyrazoline nucleus represent an important core for triaryl substituted derivatives such as compound **1** (**Fig. 1**) that had been reported to exhibit powerful cytotoxic activity against different cancer cell lines [27]. In addition, the strategy of hybridization of pyrazoline core with different heterocyclic nuclei such as thiophene (compound **2**) [18] and pyrimidine (compound **3**) [17] proved effective in production of potent antiproliferative analogs. Therefore, the pyrazoline ring is an advantageous choice for the synthesis of pharmaceutical compounds with diverse biological activities and good safety profiles [28-30]. On the other hand, pyridazine is considered a significant group of heterocyclic compounds which contains two adjacent nitrogen atoms. In recent years, there has been an

increasing interest in the pyridazine ring system due its diverse biological activities and other beneficial applications [31, 32]. Various pyridazine derivatives have been reported to possess increasing attention in the synthesis and evaluation of their biological properties. This indicates that various substituted pyridazine compounds possess different types of pharmacological activities, such as antidiabetic [33], antimicrobial [34], antihypertensive [35], anti-inflammatory [36], and antiproliferative agents [37-40]. Pyridazine **4** (**Fig. 1**) revealed promising cytotoxic activity [41]. A series of novel compounds containing the pyridazine moiety were reported as potent anticancer agents targeting EGFR tyrosine kinase [42]. Finally, from the molecular design point of view, the combination of two pharmacophores into one single molecule represents one of the most important methods that can be used to synthesize new anticancer molecules [43-45].

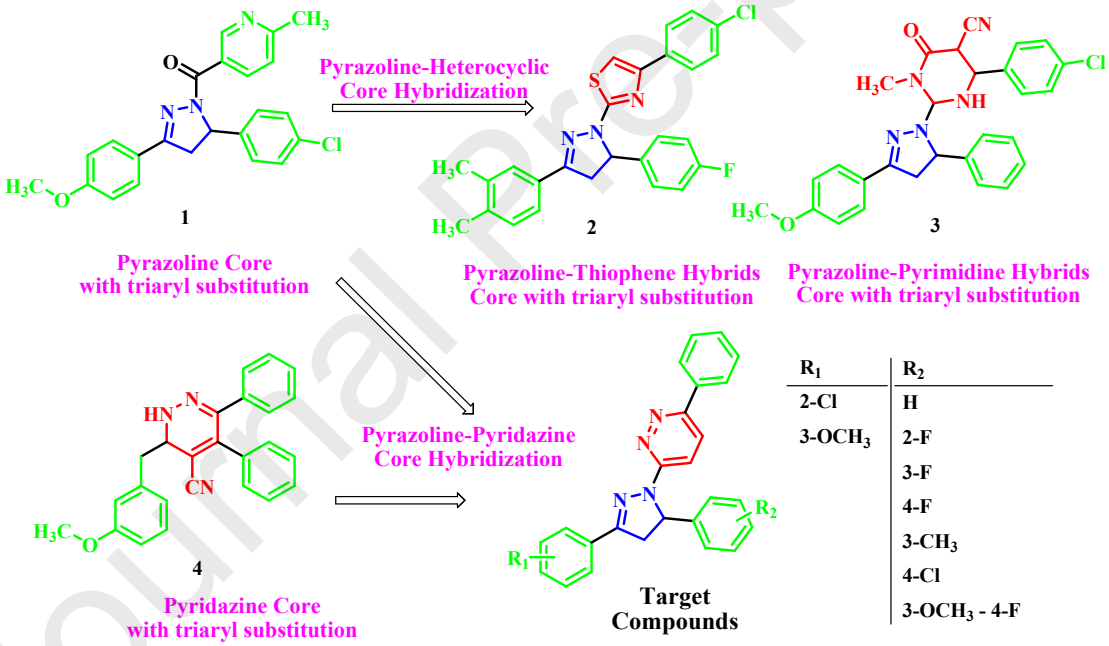

Fig. 1. Structures of reported antiproliferative compounds with heterocyclic core and triaryl substitution and the structure of the target pyrazoline-pyridazines core hybridization.

This work therefore adopted the hybridization of pyrazoline and pyridazine core with triaryl substitution for the synthesis of a novel pyrazoline/pyridazine hybrids **IXa-n**, aiming to obtain new promising antiproliferative compounds (**Fig. 1**). The newly synthesized target compounds were sent to the National Cancer Institute (NCI) for assessment of their anticancer activity. Additionally, the most active candidates have

been tested against target EGFR tyrosine kinase inhibition. Also, this study determined annexin V-FITC apoptosis assay. Moreover, the cell cycle activity was detected for the most potent compounds, to get an overview about the possible stage at which the new derivatives could suppress the growth of cancer cells. Furthermore, levels of Bax, Bcl2 and caspase-3 was also determined in this study.

2. Results and discussion

2.1. Chemistry

Compound **III** was prepared via the reaction of acetophenone **I** with glyoxilic acid **II** in the presence of hydrazine hydrate [46]. Furthermore, the reaction between phosphorous oxychloride and compound **III** afford 3-chloropyridazine **IV** which has been reacted with hydrazine hydrate to obtain **V** (**Scheme 1**) [47].

On the other hand, Chalcones derivatives **VIIIa-n** were prepared by the Claisene Schmidt condensation between acetophenones **VIa** or **VIb** and appropriate aldehyde derivatives **VII** [48-57]. Finally, the target compounds **IXa-n** were prepared by reaction of **V** with the appropriate chalcones **VIII a-n** in absolute ethanol and in the presence of sodium hydroxide (**Scheme 1**). All the final compounds **IXa-n** were characterized by IR, MS, ^{1}HNMR, ^{13}CNMR and elemental analysis.

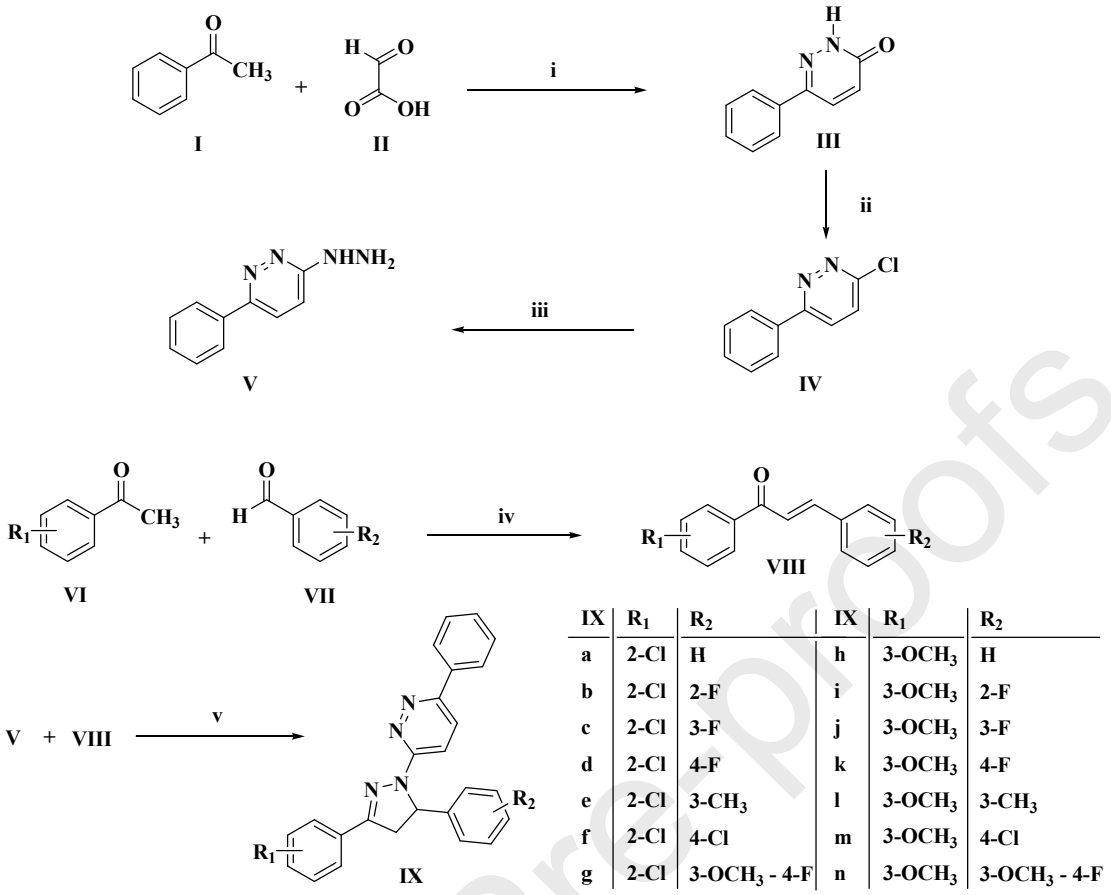

IX	R_1	R_2	IX	R_1	R_2
a	2-Cl	H	h	3-OCH_3	H
b	2-Cl	2-F	i	3-OCH_3	2-F
c	2-Cl	3-F	j	3-OCH_3	3-F
d	2-Cl	4-F	k	3-OCH_3	4-F
e	2-Cl	3-CH_3	l	3-OCH_3	3-CH_3
f	2-Cl	4-Cl	m	3-OCH_3	4-Cl
g	2-Cl	3-OCH_3 - 4-F	n	3-OCH_3	3-OCH_3 - 4-F

Scheme 1: Synthesis of compounds **IXa-n;** Reagents and conditions: (**i**) hydrazine hydrate, EtOH, reflux, 4h; (**ii**) phosphorous oxychloride, reflux, 2h; (**iii**) hydrazine hydrate, EtOH, reflux, 10h.; (**iv**) ethanolic NaOH, r.t. 6h; (**v**) ethanolic NaOH, reflux, 15h.

2.2 Biological activity

2.2.1. Screening of anticancer activity and SAR discussion:

Data analysis showed that most synthesized compounds demonstrated different level of growth inhibition against the nine panels of tumor cell lines (**Table 1 and 2**). Furthermore, cell lines of ovarian cancer IGROV1, breast cancer T-47D, renal cancer CAKI-1 and UO-31 were sensitive to almost all evaluated compounds. In this study, we have two series of compounds, first series bearing Cl moiety at position 2 (lead compound **IXa**), the other series bearing methoxy group at position 3 (lead compound **IXh**). Structure–activity correlation was based on the obtained results and in comparison, to the lead compounds, **IXa** and **IXh** by introducing different aryl moieties at 5-position of pyrazole moiety.

The first series, lead compound **IXa** with phenyl moiety at position 5 displayed cell growth inhibition for ovarian cancer IGROV1 (30.19%), renal cancer CAKI-1 (38.28%), renal cancer UO-31 (34.60%), and breast cancer T-47D (41.75%). Substitution with flouro group at position 2 of the phenyl moiety **IXb** increase selectivity against renal cancer CAKI-, renal cancer UO-31, and breast cancer T-47D with growth inhibition (51.05%, 39.54%, 49.22%) respectively.

On the other hand substitution with flouro group at position 3 **IXc** increase selectivity on renal cancer CAKI-1 and UO-31 with cell growth inhibition 40.10%, 46.04%, while substitution with flouro group at position 4 **IXd** shows marked increase growth inhibition against ovarian cancer OVCAR-4 (46.44%), renal cancer CAKI-1 (62.98%), renal cancer UO-31 (51.58%), breast cancer T-47D (55.56%). Compound **IXe** with 3 methyl group at position 3 show only increase in sensitivity toward renal cancer UO-31 (cell growth inhibition: 46.54%). Compound **IXf** with Cl moiety at position 4 decreased in sensitivity toward ovarian cancer IGROV1, breast cancer T-47D, renal cancer CAKI-1, UO-31, cell lines. Furthermore compound **IXg** with flouro group at position 4 and methoxy group at position 3 of the phenyl moiety show marked increase in cell growth inhibition of ovarian cancer IGROV1 (47.17%), renal cancer CAKI-1 (45.86%), renal cancer UO-31 (49.22%).

Table 1: In vitro antiproliferative activity results of compounds **IXa - IXg** against sixty human tumor cell lines; results were provided as a percentage of cell growth promotion.

Panel	Subpanel	IXa	IXb	IXc	IXd	IXe	IXf	IXg
Leukemia	CCRF-CEM	95.17	93.16	98.76	81.77	98.56	98.99	107.00
	HL-60(TB)	98.84	103.32	96.07	92.04	91.22	108.66	95.37
	K-562	81.65	88.71	87.85	65.68	81.57	95.98	88.97
	MOLT-4	81.48	81.35	88.11	56.77	87.58	94.93	82.30
	RPMI-8226	87.78	86.37	92.61	64.11	85.27	94.73	92.04
	SR	77.36	81.35	87.07	75.76	82.51	85.40	83.78
Non-small cell lung cancer	A549/ATCC	90.54	96.50	92.13	77.62	88.47	98.96	88.83
	EKVX	90.78	89.85	82.98	77.68	84.38	93.69	79.42
	HOP-62	90.19	89.08	88.15	84.10	94.55	91.65	86.29
	HOP-92	87.29	78.90	75.41	79.79	79.65	94.24	76.02
	NCI-H226	87.45	89.73	81.97	74.29	86.45	91.77	77.67
	NCI-H23	95.44	91.38	94.12	77.87	85.96	98.53	86.56
	NCI-H322M	96.73	99.26	97.98	95.68	100.53	103.83	100.12
	NCI-H460	97.59	97.96	98.02	87.15	88.14	99.42	97.57
	NCI-H522	84.59	85.27	84.31	69.25	80.86	96.21	88.20

Colon cancer	COLO 205	100.76	107.11	105.93	91.34	81.80	104.77	97.59
	HCC-2998	102.88	103.70	106.01	99.42	94.09	98.82	102.10
	HCT-116	81.35	80.60	85.92	57.66	69.17	93.94	80.33
	HCT-15	92.20	90.15	100.53	81.24	91.25	106.80	98.59
	HT29	80.69	91.78	85.12	69.48	58.71	101.87	81.63
	KM12	94.17	99.92	96.77	78.34	92.58	97.67	92.94
	SW-620	97.48	94.98	91.23	85.94	89.23	98.75	89.65
CNS cancer	SF-268	92.58	87.69	91.12	74.16	83.15	92.14	87.11
	SF-295	101.96	99.04	100.12	86.94	101.02	101.28	99.90
	SF-539	93.55	92.61	94.46	83.32	96.72	98.98	95.30
	SNB-19	94.08	90.07	92.93	83.90	88.94	100.18	94.82
	SNB-75	88.73	68.90	86.82	76.41	66.06	65.63	68.24
	U251	89.79	87.90	89.45	77.22	84.36	92.82	90.24
Melanoma	MALME-3M	91.78	92.61	92.19	86.84	88.58	95.15	94.52
	M14	92.66	91.42	97.55	76.90	87.96	96.19	94.32
	MDA-MB-435	100.91	100.74	101.44	96.33	98.06	101.20	98.94
	SK-MEL-2	101.65	102.71	107.21	93.70	97.30	114.51	102.37
	SK-MEL-28	98.77	101.52	104.43	95.62	101.89	106.58	102.97
	SK-MEL-5	85.36	90.05	89.89	78.17	84.12	90.08	79.05
	UACC-257	105.77	100.44	101.79	100.23	98.22	103.78	95.92
	UACC-62	81.50	74.53	78.60	72.37	76.15	89.63	82.50
Ovarian cancer	IGROV1	69.81	73.86	66.17	58.39	68.46	85.40	52.83
	OVCAR-3	100.31	97.84	98.08	72.38	92.77	97.26	80.63
	OVCAR-4	80.47	81.84	83.29	53.56	79.22	97.44	80.94
	OVCAR-5	103.28	96.41	98.22	98.63	100.68	101.42	99.38
	OVCAR-8	93.50	91.45	94.93	80.87	83.56	97.83	89.39
	NCI/ADR-RES	92.60	87.92	94.04	81.18	86.84	101.30	89.19
	SK-OV-3	90.39	96.86	87.85	78.50	83.71	97.73	83.00
Renal cancer	786-0	92.86	97.68	100.17	89.38	89.35	105.45	94.91
	A498	78.45	82.57	90.80	79.34	84.79	103.84	88.26
	ACHN	99.31	94.76	95.97	83.88	95.03	101.48	90.37
	CAKI-1	61.72	48.95	59.90	37.02	60.37	64.66	54.14
	RXF 393	98.54	88.25	98.64	88.06	93.25	109.71	96.45
	SN12C	92.49	91.46	91.61	79.67	92.87	94.68	97.66
	TK-10	103.62	111.44	131.33	130.89	108.60	146.06	151.25
	UO-31	65.40	60.46	53.96	48.42	53.46	67.36	50.78
Prostate cancer	PC-3	76.29	76.87	76.75	56.88	71.43	91.59	71.05
	DU-145	105.04	102.57	106.17	91.83	99.00	109.86	96.85
Breast cancer	MCF7	80.57	82.85	84.78	66.25	80.42	95.27	82.33
	MDA-MB-231/ATCC	89.09	77.05	85.11	75.21	91.55	92.22	91.95
	HS 578T	93.32	93.84	89.59	80.00	94.30	100.42	91.86
	BT-549	95.54	98.34	95.11	87.39	94.01	97.55	95.15
	T-47D	58.25	50.78	73.51	44.44	61.76	69.53	60.67
	MDA-MB-468	96.89	102.35	107.89	79.02	97.37	113.45	99.70

On the other hand, the second series, lead compound **IXh** displayed cell growth inhibition for ovarian cancer IGROV1, renal cancer CAKI-1, renal cancer UO-31 and breast cancer T-47D (47.11%, 33.37%, 41.31%, 20.31%) respectively. Substitution with flouro group at position 2 of the phenyl moiety **IXi** increase selectivity against

renal cancer CAKI-1 (cell growth inhibition: 49.73%), while substitution with flouro group at position 3 **IXj** increase cell growth inhibition of renal cancer UO-31 (47.27%). Furthermore, compounds **IXk** (with flouro moiety at position 4) **IXl** (with methyl moiety at position 3)**,** and **IXm** (with Cl moiety at position 4) show decreased in sensitivity toward ovarian cancer IGROV1, breast cancer T-47D, renal cancer CAKI-1and UO-31, cell lines. Compound **IXn** with flouro group at position 4 and methoxy group at position 3 of the phenyl moiety show increase in cell growth inhibition for renal cancer UO-31 (35.44%), breast cancer T-47D (59.08%).

Table 2: In vitro antiproliferative activity results of compounds **IXh - IXn** against sixty human tumor cell lines; results were provided as a percentage of cell growth promotion.

Panel	Subpanel	IXh	IXi	IXj	IXk	IXl	IXm	IXn
Leukemia	CCRF-CEM	99.59	95.14	96.27	99.70	96.26	90.56	94.47
	HL-60(TB)	101.11	104.71	86.76	98.66	103.81	87.37	97.89
	K-562	92.60	88.84	83.25	96.80	87.33	84.32	84.03
	MOLT-4	90.64	76.66	80.54	96.78	86.48	82.54	82.21
	RPMI-8226	97.99	87.99	81.10	104.50	89.85	78.08	80.57
	SR	95.27	82.32	78.32	86.70	82.86	79.14	84.67
Non-small cell lung cancer	A549/ATCC	93.99	88.73	85.57	96.99	94.54	91.02	95.14
	EKVX	NT	76.41	83.81	91.46	82.79	83.26	86.73
	HOP-62	79.40	81.98	95.20	91.27	89.82	90.71	99.67
	HOP-92	77.68	70.54	75.85	87.34	85.08	91.47	93.01
	NCI-H226	71.14	74.42	82.55	89.69	85.03	85.24	92.93
	NCI-H23	90.40	86.20	89.19	92.08	85.75	82.20	89.90
	NCI-H322M	85.48	88.64	92.34	92.98	91.18	96.54	101.50
	NCI-H460	97.28	94.38	97.79	99.28	97.71	88.38	96.79
	NCI-H522	93.49	86.51	80.65	94.34	89.29	83.83	91.48
Colon cancer	COLO 205	106.93	107.55	94.30	107.01	99.73	88.30	96.53
	HCC-2998	98.98	105.04	98.51	100.56	103.84	97.28	105.27
	HCT-116	80.09	80.57	82.45	100.80	81.78	68.22	68.24
	HCT-15	NT	94.95	85.39	100.15	88.59	85.74	91.02
	HT29	100.76	93.14	83.66	102.06	91.00	67.28	82.86
	KM12	96.87	87.20	92.78	98.68	97.31	89.32	93.00
	SW-620	93.34	89.46	90.80	100.04	92.62	82.00	92.26
CNS cancer	SF-268	86.68	88.64	85.33	93.75	90.92	87.19	91.28
	SF-295	NT	95.42	101.51	101.06	95.61	100.22	100.24
	SF-539	93.49	94.57	91.44	94.45	94.79	95.74	96.31
	SNB-19	87.63	87.70	82.17	91.94	87.85	87.68	92.84
	SNB-75	91.83	78.85	82.99	83.87	98.18	78.34	103.49
	U251	91.13	90.61	86.21	97.04	92.25	84.53	90.87
Melanoma	MALME-3M	84.38	93.28	88.39	97.34	95.19	93.94	100.96
	M14	87.93	91.33	88.74	102.05	88.90	85.99	94.59
	MDA-MB-435	101.22	100.95	99.98	102.04	100.83	97.92	100.87
	SK-MEL-2	102.59	98.46	83.75	105.21	97.46	94.64	98.06

	SK-MEL-28	99.68	105.33	98.38	103.04	101.89	98.85	106.00
	SK-MEL-5	88.62	91.86	89.43	98.36	98.22	94.52	84.86
	UACC-257	96.56	98.35	96.58	108.24	99.92	98.01	104.54
	UACC-62	75.70	73.07	77.23	94.59	75.52	79.65	86.96
Ovarian cancer	IGROV1	52.89	61.59	57.14	89.38	72.10	72.62	85.75
	OVCAR-3	91.33	91.72	89.90	106.96	99.90	96.92	100.73
	OVCAR-4	93.48	82.61	84.39	99.68	85.46	89.54	76.78
	OVCAR-5	95.02	98.16	92.50	99.58	90.35	96.34	100.07
	OVCAR-8	94.23	93.71	87.66	99.54	93.71	89.08	93.38
	NCI/ADR-RES	92.91	94.32	86.23	101.68	95.01	93.79	95.24
	SK-OV-3	84.91	89.75	85.32	96.28	92.99	79.34	100.10
Renal cancer	786-0	102.02	106.26	86.19	99.25	100.25	89.56	98.43
	A498	57.41	78.32	66.28	79.22	76.01	75.27	76.08
	ACHN	87.47	87.51	90.98	98.65	97.95	95.81	101.58
	CAKI-1	66.63	50.27	68.52	79.54	65.27	71.06	73.33
	RXF 393	91.73	102.26	85.00	96.96	92.08	98.11	110.69
	SN12C	91.35	90.47	89.07	93.20	88.15	98.59	101.32
	TK-10	145.99	170.13	131.49	125.03	143.16	137.87	109.39
	UO-31	58.69	62.38	52.73	85.86	75.67	67.82	64.56
Prostate cancer	PC-3	84.53	79.65	73.51	100.02	85.93	71.20	78.78
	DU-145	101.12	102.87	100.08	102.87	98.84	99.93	102.32
Breast cancer	MCF7	NT	83.96	79.82	93.95	82.71	76.22	85.62
	MDA-MB-231/ATCC	74.15	78.02	86.48	86.96	77.70	85.54	97.06
	HS 578T	94.46	81.30	88.48	95.79	95.78	85.05	94.14
	BT-549	88.41	91.37	93.30	96.65	94.15	91.63	97.45
	T-47D	79.69	74.00	77.44	99.94	85.94	72.82	40.92
	MDA-MB-468	89.67	97.15	92.35	100.47	99.54	99.50	95.35

NT: Not tested.

2.2.2. IC_{50} determination of the synthesized compounds against EGFR

All new synthesized compounds **IXa-n** were further investigated for their inhibitory effect on human EGFR using Erlotinib as a positive control to determine their IC_{50} values as shown in (**Table 3**). The tested compounds showed significant inhibitory effect (IC_{50}=5.5–0.65 µM). It was found that compounds **IXn**, **IXg**, **IXb** and **IXl** inhibition effect more than Erlotinib towards EGFR (IC_{50}=0.65, 0.75, 0.82 and 0.84 µM, respectively) compared to Erlotinib (IC_{50}=0.95 µM). Compound **IXc** had the same potency as Erlotinib against EGFR.

Table 3: Inhibition activities of compounds **IXh - IXn** against EGFR.

Comp.	EGFR IC_{50} (µM)
IXa	2.1 ± 0.12
IXb	0.82 ± 0.06
IXc	0.95 ± 0.07

IXd	3.7 ± 0.26
IXe	3.9 ± 0.2
IXf	4.8 ± 0.25
IXg	0.75 ± 0.05
IXh	1.7 ± 0.14
IXi	5.5 ± 0.41
IXj	4.1 ± 0.3
IXk	5.3 ± 0.43
IXl	0.84 ± 0.06
IXm	3.1 ± 0.23
IXn	0.65 ± 0.03
Erlotinib	0.95 ± 0.08

2.2.3. Cell cycle analysis

Results in **Tables 1** and **2** revealed that compounds **IXg** and **IXn** exhibited potent cytotoxic activity towards renal cancer cell line UO-31. In this manner, the effect of both compounds on the cell cycle progression of UO-31 cancer cells were performed to carry out preliminary mechanistic studies of their anticancer activity. The cancer cells were incubated for 24 h with compounds **IXg** and **IXn** at 10 µM. Results analysis indicated that both compounds resulted in increased of cell numbers in phase G2/M (50.11 % vs. 45.26 % and 12.39 %), suggesting that cell cycle was arrested in phase G2/M (**Table 4, Fig. 2**).

Table 4: Effect of compounds **IXg** and **IXn** on the cell cycle progression of UO-31 cells.

Code	%G0/G1	%S	%G2/M	%Pre-G1	Comment
IXg/ UO-31	24.45	25.44	50.11	20.17	Cell growth arrest@G2/M
IXn/ UO-31	28.14	26.6	45.26	15.36	Cell growth arrest@G2/M
Cont. **(UO-31)**	51.28	36.33	12.39	1.85	

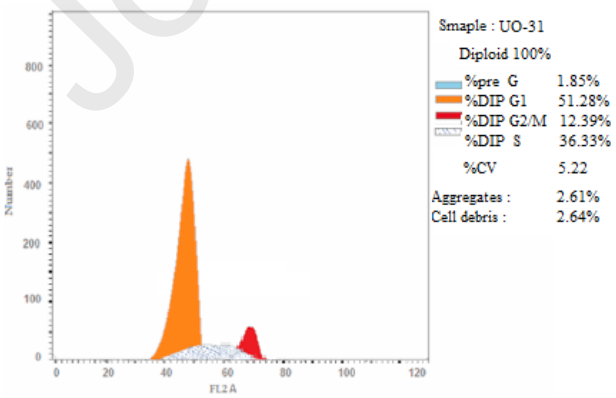

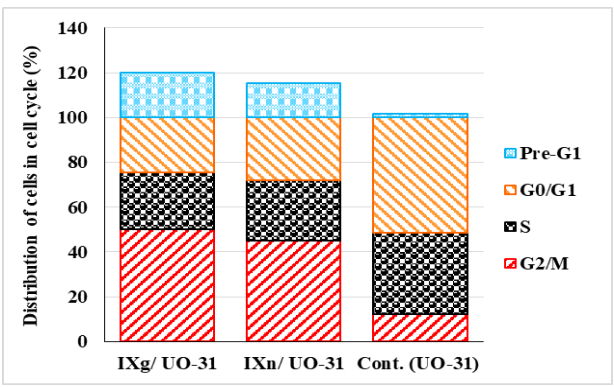

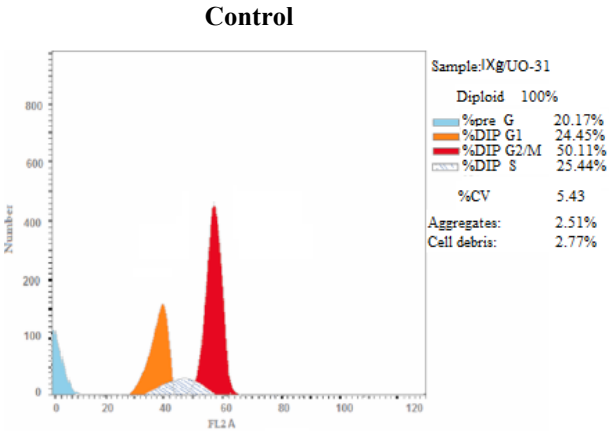

Fig. 2. Cell cycle analysis and apoptosis effect in **UO-31** cell line when treated with compounds **IXg** and **IXn**.

2.2.4. Annexin V-FITC apoptosis assay

Cell cycle assay of UO-31 cancer cells treated with compounds **IXg** and **IXn** showed pre-G1 peak appearance which emphasized apoptosis induction. The cells were stained with Annexin V / PI, incubated for 24 h and analyzed to confirm the efficacy of these compounds to cause apoptosis. It has been found that the early and late apoptosis induced by the compounds being studied definitely suggested their ability to cause meaningful apoptosis rates with 1.5 and 2.7 % necrosis respectively (**Table 5, Fig. 3**). In addition, the percentages of late apoptosis (10.29% and 7.25%) induced by **IXg** and **IXn** were higher than those of early apoptosis (8.37% and 5.41%) which makes recovery of apoptotic cells more difficult to be healthy.

Table 5. Induced apoptosis and necrosis on UO-31 cells by **IXg** and **IXn**.

	Apoptosis			Necrosis
	Total	**Early**	**Late**	
IXg/UO-31	20.17	8.37	10.29	1.51
IXn/UO-31	15.36	5.41	7.25	2.7
Cont. (UO-31)	1.85	1.13	0.29	0.43

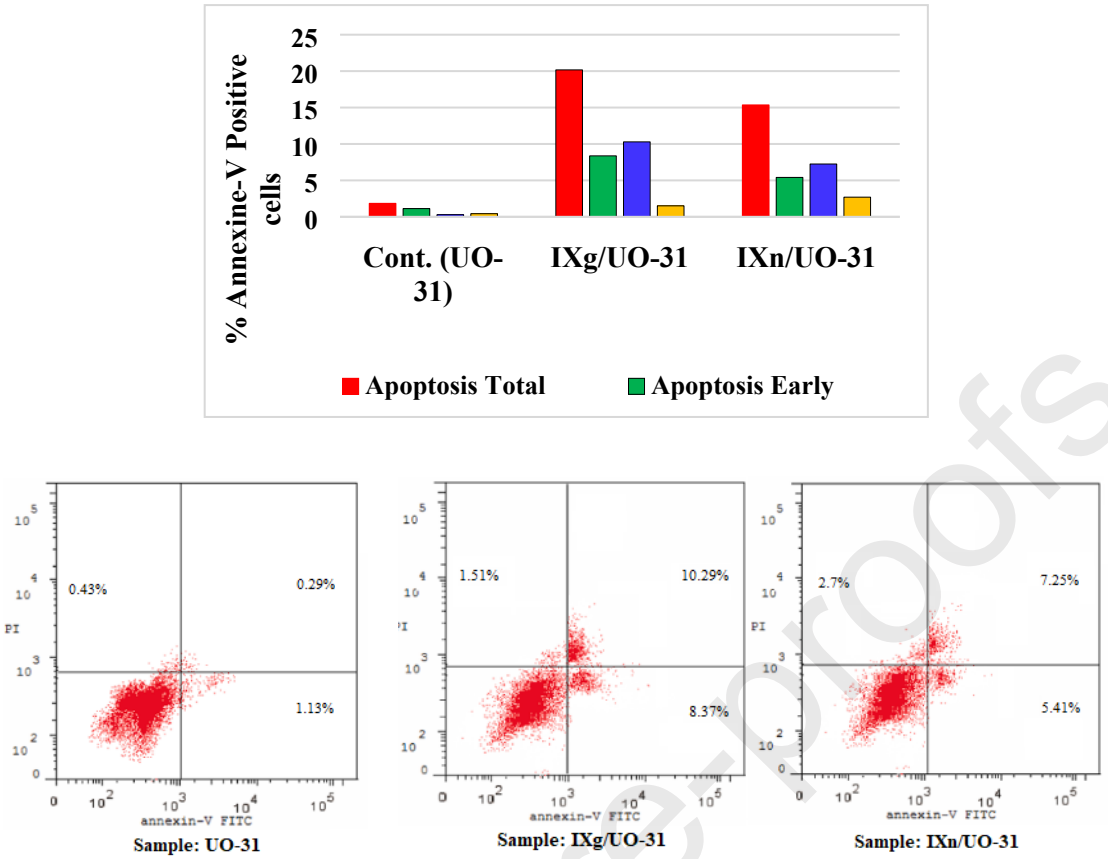

Fig. 3. Effect of compounds **IXg** and **IXn** on the percentage of V-FITC-positive annexin staining in UO-31 cells.

2.2.5. Effects on the levels of Bax, Bcl-2 and active caspase-3

Apoptosis is regulated by various factors including stimulation of the apoptotic pathway through caspase-3, inducers (Bax protein) and suppressors (Bcl-2 protein) [58]. The key members of apoptotic pathways are the cysteine protease caspase family [59]. Caspase-3 is an apoptosis executioner and that its activation contributes to apoptosis induction [58]. Many studies on human cancers have revealed a relationship between increased Bcl-2 levels, decreased Bax levels and uncontrolled cell growth [59, 60]. Therefore, in this study, the levels of Bcl-2, Bax and caspase-3 were determined after treatment with **IXg** and **IXn** in UO-31cells in order to examine the effect of both compounds on these apoptotic biomarkers. The findings presented in (**Table 6**) showed that **IXg** and **IXn** raised the Bax level by 7.3 and 6.6 folds, respectively, and decreased the Bcl-2 level by 0.31 and 0.44 folds, respectively, compared with the control. Also results showed that the active caspase-3 was significantly overexpressed by 7.1 and 5.9 folds relative to the control indicating the apoptosis induction potential of these compounds.

Table 6. Bax, Bcl2 and Caspase-3 analysis results after treatment with compound **IXg** and **IXn**.

Comp.	Bax conc. pg	FLD	Bcl-2 Conc. pg	FLD	Caspase-3 conc. pg	FLD
13	392.17	7.33	1.84	0.317	419.25	7.19
14	356.25	6.6	2.56	0.44	347.11	5.95
Cont.	53.49	1	5.79	1	58.31	1

2.3. Molecular docking

Molecular docking studies are an important method for studying molecular interactions between the synthesized ligands and main amino acids at the respective protein binding site [61]. Ligand – protein interaction activity at the binding active site was measured on the basis of the docking score values determined using MOE 2015.10. In the present research, all synthesized compounds were subjected to molecular modeling studies using MOE software on the EGFR 3D structure and using Erlotinib as a reference compound Table 7, in order to predict the behavior of the synthesized compounds as an anticancer agents. The results of the docking studies showed that the binding free energy of the compounds being examined exhibited favorable docking complexes with the active target protein site. The compounds being studied displayed interactions with the active EGFR sites with the same amino acid as did the reference drug, Erlotinib. Although, all the tested compounds showed significant docking score free energy compared to Erlotinib, compounds **IXc**, **IXg**, **IXj**, **IXe**, and **IXn** showed the best docking score free energy (**Table 7**).

Table 7. Docking energy scores (kcal/mol) derived from the MOE for Compounds **IXa-n** and **Erlotinib**.

Comp. No.	Score	rmsd_ refine	E_conf	E_place	E_score1	E_refine	E_score2
IXa	-7.5032	1.1158	52.5396	-67.4750	-13.0213	-43.1217	-7.5032
IXb	-7.4828	1.1512	52.4754	-82.2369	-12.2609	-35.5909	-7.4828
IXc	-8.0715	1.5914	46.3532	-53.7557	-11.9093	-42.3909	-8.0715
IXd	-7.5669	1.2320	52.2871	-76.9072	-13.2147	-41.1207	-7.5669
IXe	-7.6098	1.1562	50.0204	-99.3674	-11.9157	-40.4771	-7.6098
IXf	-7.5063	2.3522	49.8316	-71.1179	-12.5182	-43.0492	-7.5063
IXg	-7.7437	1.2496	70.0082	-93.1728	-12.3985	-37.4756	-7.7437
IXh	-7.4173	2.0378	61.9342	-66.4482	-12.0435	-40.5859	-7.4173

IXi	-7.4513	1.1826	55.3965	-67.8661	-11.5407	-38.7661	-7.4513
IXj	-7.6264	1.1773	62.3024	-58.6817	-12.0223	-41.9693	-7.6264
IXk	-7.4602	1.9206	64.0970	-66.7235	-12.1795	-40.9835	-7.4602
IXl	-7.4967	1.9904	62.7921	-66.7189	-11.4621	-39.5500	-7.4967
IXm	-7.4797	1.3109	55.0005	-86.0764	-13.1680	-38.6300	-7.47977
IXn	-7.5941	1.8792	78.2140	-68.6826	-12.3753	-40.3379	-7.5941
Erlotinib	-7.3430	2.9191	-34.3322	-71.5678	-12.4086	-42.4795	-7.3430

Score; lower scores are more favorable, **rmsd_refine**; the root mean square deviation of the pose from the docking pose compared to the co-crystal ligand position, **E_conf**; free binding energy of the conformer, **E_place**; free binding energy from the placement stage, **E_score 1**; free binding energy from the first rescoring stage, **E_refine**; free binding energy from the refinement stage, **E_score 2**; free binding energy from the second rescoring stage.

Compound **IXg** and **IXn** showed an excellent docking score (-7.7437 kcal/mol and -7.5941 kcal/mol) compared to **Erlotinib** docking score (-7.3430 kcal/mol), and both formed a direct interaction with most of the amino-acids that **Erlotinib** interacted with. Where, **Erlotinib** had a direct interaction with amino-acids **VAL702**, **LYS721**, **CYS751** and **THR766** in the active site (**Fig. 4A**), compound **IXg** and **IXn** showed interactions with amino-acids **LEU694**, **LYS721** and **THR766** in the active site (**Fig4 4B and 4C**). Also, compounds **IXg** and **IXn** showed high degrees of superimposition **Erlotinib** into EGFR active sites (**Fig. 4B and 4C**). These results were in a perfect match with the **EGFR** enzyme inhibition assay where compounds **IXg** and **IXn** had IC_{50s} of (0.75 µM/mL and 0.65 µM/mL, respectively) compared to that of **Erlotinib** (0.95 µM/mL) (**Table 3**).

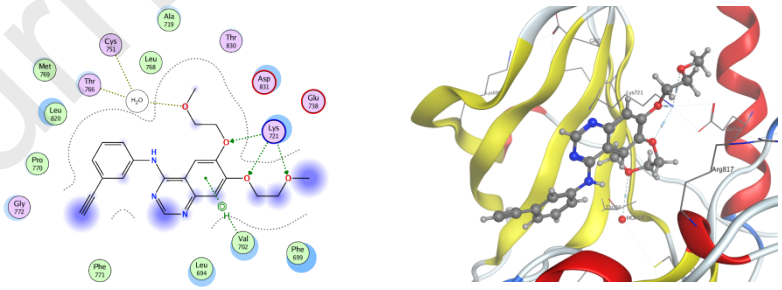

A) Interaction of **Erlotinib** with amino-acids VAL702, LYS721, CYS751 and THR766.

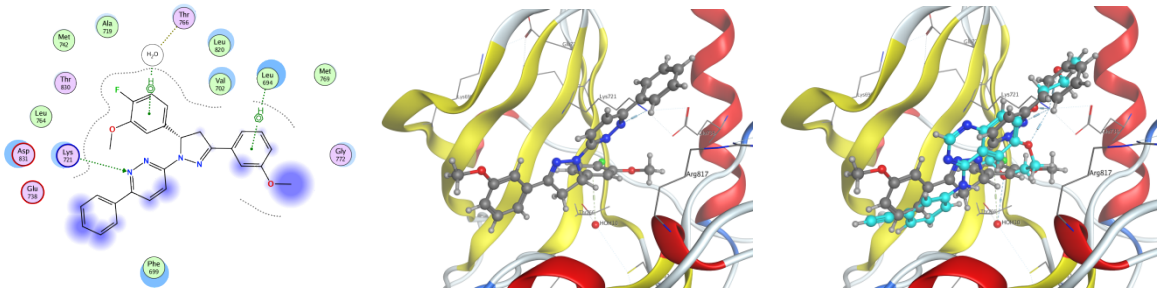

B) Interaction of **IXg** with amino-acids LEU694, LYS721 and THR766 and superimposition of **IXg** (shown as grey sticks) with **Erlotinib** (shown as cyan sticks).

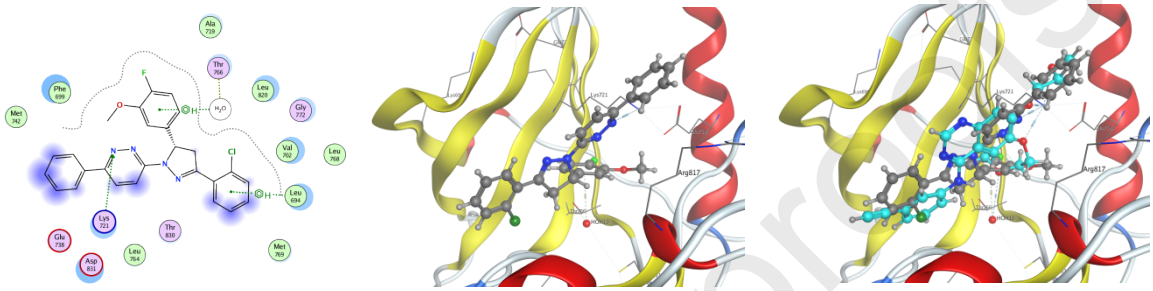

C) Interaction of **IXn** with amino-acids LEU694, LYS721 and THR766 and superimposition of **IXn** (shown as grey sticks) with **Erlotinib** (shown as cyan sticks).

Fig. 4. Docking of compounds **IXg, IXn** and **Erlotinib** into EGFR active sites.

3. Experimental

3.1. Chemistry

IR spectra had been measured on a Perkin Elmer-9712 spectrophotometer. Elemental microanalysis was performed at the Micro-analytical Laboratory at Cairo University, Egypt. ^{1}H NMR spectrometer and ^{13}C NMR spectra were measured on Bruker 400 MHz NMR. For the evaluation of mass spectra, a Shimadzu Qp-2010 Plus was used. 6-phenylpyridazines **V** [46, 47] and Chalcones **VIII** [48-57] have been prepared according to the procedures indicated.

3.1.1. General procedure for preparation of IXa-n

In absolute ethanol (15 mL), a mixture of the corresponding chalcones **VIIIa-n** (1 mmol), hydrazine derivatives **V** (1 mmol) and sodium hydroxide (2.5 mmol) were heated for 15 h under reflux. Filtered and washed with water and crystallized with ethanol.

3.1.1.1. 3-(3-(2-chlorophenyl)-4,5-dihydro-5-phenylpyrazol-1-yl)-6-phenyl-pyridazine (IXa)

White powder (yield 64%); m.p. 107-109 ^{o}C; IR ($\upsilon_{max.}$/cm^{-1}) 3031 (C-H aromatic), 1649 (C=N) and at 1588 (C=C); ^{1}HNMR (400 MHz, DMSO-d$_6$) δ *ppm*: 8.08 (d, *J* = 9.3 Hz, 1H, Ar-H), 8.00 (d, *J* = 7.6 Hz, 2H, Ar-H), 7.81-7.85 (m, 1H, Ar-H), 7.78 (d, *J* = 9.5 Hz, 1H, Ar-H), 7.56-7.60 (m, 1H, Ar-H), 7.41-7.50 (m, 6H, Ar-H), 7.30-7.36 (m, 4H, Ar-H), 5.94 (dd, *J* = 5.1, 12.0 Hz, 1H, pyrazoline-CH), 4.16 (dd, *J* = 12.0, 17.9 Hz, 1H, one proton of pyrazoline-CH$_2$), 3.31 (d, *J* = 5.4 Hz, 1H, one proton of pyrazoline-CH$_2$); ^{13}CNMR (100 MHz, DMSO-d$_6$) δ *ppm*: 155.9, 152.4, 151.1, 142.9, 136.8, 131.9, 131.4, 131.2, 131.1, 130.7, 129.4, 129.3, 129.2, 127.9, 127.7, 126.7, 126.3, 126.2, 115.4, 62.1, 45.7; MS (m/z (R.I. %)); [M]$^{+}$ 410 (12.7), [M+2]$^{+}$ 412 (4.7), 272 (100), 170 (17.4); Anal. Calcd. for $C_{25}H_{19}ClN_4$ (410.13); % C, 73.08; H, 4.66; N, 13.64, Found: % C, 73.21; H, 4.75; N, 13.71.

3.1.1.2. 3-(3-(2-chlorophenyl)-5-(2-fluorophenyl)-4,5-dihydropyrazol-1-yl)-6-phenyl-pyridazine (IXb)

White powder (yield 60%); m.p. Over 280 ^{o}C; IR ($\upsilon_{max.}$/cm^{-1}) 3054 (C-H aromatic), 1649 (C=N) and at 1589 (C=C); ^{1}HNMR (400 MHz, DMSO-d$_6$) δ *ppm*: 8.10 (d, *J* = 9.5 Hz, 1H, Ar-H), 8.00 (d, *J* = 7.6 Hz, 2H, Ar-H), 7.82-7.86 (m, 1H, Ar-H), 7.79 (d, *J* = 9.3 Hz, 1H, Ar-H), 7.55-7.61 (m, 1H, Ar-H), 7.42-7.50 (m, 5H, Ar-H), 7.29-7.34 (m, 1H, Ar-H), 7.20-7.28 (m, 2H, Ar-H), 7.13 (t, *J* = 7.3 Hz, 1H, Ar-H), 6.09 (dd, *J* = 5.6, 12.2 Hz, 1H, pyrazoline-CH), 4.19 (dd, *J* = 12.4, 17.7 Hz, 1H, one proton of pyrazoline-CH$_2$), 3.30 (m, 1H, one proton of pyrazoline-CH$_2$); MS (m/z (R.I. %)); [M]$^{+}$ 428 (25.5), [M+2]$^{+}$ 430 (9.7), 290 (79.5), 272 (100), 170 (31.2); Anal. Calcd. For $C_{25}H_{18}ClFN_4$ (428.12); % C, 70.01; H, 4.23; N, 13.06, Found: % C, 70.09; H, 4.35; N, 13.15.

3.1.1.3. 3-(3-(2-chlorophenyl)-5-(3-fluorophenyl)-4,5-dihydropyrazol-1-yl)-6-phenylpyridazine (IXc)

Yellowish powder (yield 59%); m.p. 209-211 ^{o}C; IR ($\upsilon_{max.}$/cm^{-1}) 3064 (C-H aromatic), 1647 (C=N) and at 1590 (C=C); ^{1}H NMR (400 MHz, DMSO-d$_6$) δ *ppm*: 8.10 (d, *J* = 8.8 Hz, 1H, Ar-H), 7.97-8.04 (m, 2H, Ar-H), 7.77-7.87 (m, 2H, Ar-H), 7.57 (br. s, 1H, Ar-H), 7.44-748 (m, 6H), 7.16 (br. s, 2H, Ar-H), 7.06-7.13 (m, 1H, Ar-H), 5.87-6.03 (m, 1H, pyrazoline-CH), 4.05-4.24 (m, 1H, one proton of pyrazoline-CH$_2$), 3.32

(m, 1H, one proton of pyrazoline-CH_2); MS (m/z (R.I. %)); $[M-F]^+$ 409 (31.5), 386 (20.7), 306 (43.1), 55 (100); Anal. Calcd. for $C_{25}H_{18}ClFN_4$ (428.12); % C, 70.01; H, 4.23; N, 13.06, Found: % C, 70.12; H, 4.19; N, 12.98.

3.1.1.4. 3-(3-(2-chlorophenyl)-5-(4-fluorophenyl)-4,5-dihydropyrazol-1-yl)-6-phenyl-pyridazine (IXd)

Yellowish powder (yield 63%); m.p. 183-185 ^oC; IR ($\upsilon_{max.}/cm^{-1}$) 3038 (C-H aromatic), 1649 (C=N) and at 1588 (C=C); ^{1}HNMR (400 MHz, DMSO-d_6) δ *ppm*: 8.07 (d, *J* = 9.5 Hz, 1H, Ar-H), 8.00 (d, *J* = 7.3 Hz, 2H, Ar-H), 7.80-7.86 (m, 1H, Ar-H), 7.77 (d, *J* = 9.5 Hz, 1H, Ar-H), 7.54-7.60 (m, 1H, Ar-H), 7.41-7.50 (m, 5H, Ar-H), 7.36 (dd, *J* = 5.5, 8.0 Hz, 2H, Ar-H), 7.16 (t, *J* = 8.8 Hz, 2H, Ar-H), 5.94 (dd, *J* = 5.4, 12.0 Hz, 1H, pyrazoline-CH), 4.14 (dd, *J* = 12.2, 17.9 Hz, 1H, one proton of pyrazoline-CH_2), 3.31-3.37 (m, 1H, one proton of pyrazoline-CH_2); ^{13}CNMR (100 MHz, DMSO-d_6) δ *ppm*: 155.9, 152.5, 151.1, 136.7, 131.9, 131.4, 131.3, 131.1, 130.6, 129.4, 129.3, 128.4, 128.3, 128.0, 126.3, 126.2, 116.1, 115.8, 115.5, 61.5, 45.6; MS (m/z (R.I. %)); $[M]^+$ 428 (12.9), $[M+2]^+$ 430 (4.7), 290 (100), 170 (15.5), 115 (35.3); Anal. Calcd. for $C_{25}H_{18}ClFN_4$ (428.12); % C, 70.01; H, 4.23; N, 13.06, Found: % C, 70.09; H, 4.27; N, 13.01.

3.1.1.5. 3-(3-(2-chlorophenyl)-4,5-dihydro-5-m-tolylpyrazol-1-yl)-6-phenyl-pyridazine (IXe)

Buff powder (yield 55%); m.p. Over 280 ^oC; IR ($\upsilon_{max.}/cm^{-1}$) 3050 (C-H aromatic), 1648 (C=N) and at 1590 (C=C); ^{1}HNMR (400 MHz, DMSO-d_6) δ *ppm*: 8.08 (d, *J* = 9.3 Hz, 1H, Ar-H), 8.00 (d, *J* = 6.9 Hz, 2H, Ar-H), 7.83 (br. s, 1H, Ar-H), 7.78 (d, *J* = 9.3 Hz, 1H, Ar-H), 7.54-7.61 (m, 1H, Ar-H), 7.41-7.51 (m, 5H, Ar-H), 7.18-7.25 (m, 1H, Ar-H), 7.15 (br. s, 1H, Ar-H), 7.07 (t, *J* = 8.2 Hz, 2H, Ar-H), 5.83-5.95 (m, 1H, pyrazoline-CH), 4.15 (dd, *J* = 12.4, 17.2 Hz, 1H, one proton of pyrazoline-CH_2), 3.30 (br. s, 1H, one proton of pyrazoline-CH_2), 2.28 (s, 3H, CH_3); ^{13}CNMR (100 MHz, DMSO-d_6) δ *ppm*: 155.9, 152.4, 151.1, 143.0, 138.4, 136.7, 131.9, 131.4, 131.2, 131.1, 130.7, 129.3, 129.2, 128.4, 128.0, 126.7, 126.3, 126.2, 123.1, 115.4, 62.1, 45.8, 21.5; MS (m/z (R.I. %)); $[M]^+$ 424 (9.7), $[M+2]^+$ 426 (3.6), 286 (100), 170 (14.6), 115 (37.3)); Anal. Calcd. for $C_{26}H_{21}ClN_4$ (424.15); % C, 73.49; H, 4.98; N, 13.19, Found: % C, 73.55; H, 4.87; N, 13.25.

3.1.1.6. 3-(3-(2-chlorophenyl)-5-(4-chlorophenyl)-4,5-dihydropyrazol-1-yl)-6-phenylpyridazine (IXf)

Yellowish powder (yield 60%); m.p. Over 280 ^{o}C; IR ($\upsilon_{max.}$/cm^{-1}) 3059 (C-H aromatic), 1677 (C=N) and at 1587 (C=C); ^{1}HNMR (400 MHz, DMSO-d$_6$) δ *ppm*: 8.10 (d, *J* = 9.5 Hz, 1H, Ar-H), 8.00 (d, *J* = 7.6 Hz, 2H, Ar-H), 7.81-7.86 (m, 1H, Ar-H), 7.78 (d, *J* = 9.3 Hz, 1H, Ar-H), 7.35-7.42 (m, 6H, Ar-H), 7.11 (d, *J* = 8.1 Hz, 2H, Ar-H), 6.96 (d, *J* = 8.8 Hz, 2H, Ar-H), 5.94 (dd, *J* = 5.5, 11.9 Hz, 1H, pyrazoline-CH), 4.16 (dd, *J* = 12.2, 17.6 Hz, 1H, one proton of pyrazoline-CH$_2$), 3.33 (d, *J* = 5.6 Hz, 1H, one proton of pyrazoline-CH$_2$); ^{13}CNMR (100 MHz, DMSO-d$_6$) δ *ppm*: 155.9, 152.5, 151.2, 141.9, 138.6, 136.7, 136.3, 132.8, 131.9, 131.4, 131.2, 130.0, 129.3, 129.2, 128.3, 127.9, 126.4, 126.2, 115.4, 61.6, 45.5; MS (m/z (R.I. %)); [M]$^{+}$ 444 (9.8), [M+2]$^{+}$ 446 (6.7), 306 (100), 308 (37), 115 (50.2); Anal. Calcd. for $C_{25}H_{18}Cl_2N_4$ (444.09); % C, 67.42; H, 4.07; N, 12.58, Found: % C, 67.40; H, 3.93; N, 12.65.

3.1.1.7. 3-(3-(2-chlorophenyl)-5-(4-fluoro-3-methoxyphenyl)-4,5-dihydropyrazol-1-yl)-6-phenylpyridazine (IXg)

Buff powder (yield 64%); m.p. 166-168 ^{o}C; IR ($\upsilon_{max.}$/cm^{-1}) 3059 (C-H aromatic), 1648 (C=N) and at 1589 (C=C); ^{1}HNMR (400 MHz, DMSO-d$_6$) δ *ppm*: 8.09 (d, *J* = 9.5 Hz, 1H, Ar-H), 7.99 (d, *J* = 7.6 Hz, 2H, Ar-H), 7.81-7.86 (m, 1H, Ar-H), 7.73-7.76 (m, 2H, Ar-H), 7.33-7.37 (m, 4H, Ar-H), 7.06-7-09 (m, 2H, Ar-H), 6.94 (d, *J* = 8.8 Hz, 2H, Ar-H), 5.92 (dd, *J* = 5.6, 12.2 Hz, 1H, pyrazoline-CH), 4.14 (dd, *J* = 12.2, 17.6 Hz, 1H, one proton of pyrazoline-CH$_2$), 3.84 (s, 3H, OCH$_3$), 3.33 (d, *J* = 5.6 Hz, 1H, one proton of pyrazoline-CH$_2$); MS (m/z (R.I. %)): [M]$^{+}$ 458 (13.5), [M+2]$^{+}$ 460 (5.4), 320 (100), 197 (15.2), 115 (27); Anal. Calcd. for $C_{26}H_{20}ClFN_4O$ (458.13); % C, 68.05; H, 4.39; N, 12.21, Found: % C, 67.96; H, 4.42; N, 12.16.

3.1.1.8. 3-(4,5-dihydro-3-(3-methoxyphenyl)-5-phenylpyrazol-1-yl)-6-phenyl-pyridazine (IXh)

Buff powder (yield 60%); m.p. 162-164 ^{o}C; IR ($\upsilon_{max.}$/cm^{-1}) 2960 (C-H aromatic), 1668 (C=N) and at 1597 (C=C); ^{1}HNMR (400 MHz, DMSO-d$_6$) δ *ppm*: 8.06 (d, *J* = 8.8 Hz, 1H, Ar-H), 8.01 (d, *J* = 7.6 Hz, 2H, Ar-H), 7.80-7.84 (m, 2H, Ar-H), 7.62 (br. s, 1H, Ar-H), 7.29-7.44 (m, 6H, Ar-H), 7.16 (br. s, 2H, Ar-H), 7.01-7.8 (m, 2H, Ar-H),

5.92 (dd, *J* = 5.6, 12.2 Hz, 1H, pyrazoline-CH), 3.99 (dd, *J* = 12.2, 17.9 Hz, 1H, one proton of pyrazoline-CH_2), 3.82 (s, 3H, OCH_3), 3.31 (dd, *J* = 5.6, 17.9 Hz, 1H, one proton of pyrazoline-CH_2); MS (m/z (R.I. %)): $[M]^+$ 406 (22.5), 272 (100), 170 (14.3), 115 (26); Anal. Calcd. for $C_{26}H_{22}N_4O$ (406.18); % C, 76.83; H, 5.46; N, 13.78, Found: % C, 76.75; H, 5.42; N, 13.69.

3.1.1.9. 3-(5-(2-fluorophenyl)-4,5-dihydro-3-(3-methoxyphenyl)pyrazol-1-yl)-6-phenylpyridazine (IXi)

Yellowish powder (yield 56%); m.p. 123-125 ^oC; IR ($\upsilon_{max.}/cm^{-1}$) 3060 (C-H aromatic), 1647 (C=N) and at 1596 (C=C); ^{1}HNMR (400 MHz, DMSO-d_6) δ *ppm*: 8.08 (d, *J* = 9.3 Hz, 1H, Ar-H), 8.00 (d, *J* = 7.8 Hz, 2H, Ar-H), 7.86 (d, *J* = 9.3 Hz, 1H, Ar-H), 7.77-7.81 (m, 1H, Ar-H), 7.63 (br. s, 1H, Ar-H), 7.31-7.44 (m, 5H, Ar-H), 7.17-24 (m, 3H, Ar-H), 7.03-7.6 (m, 1H, Ar-H), 6.03 (dd, *J* = 5.5, 12.1 Hz, 1H, pyrazoline-CH), 4.04 (dd, *J* = 12.2, 17.9 Hz, 1H, one proton of pyrazoline-CH_2), 3.84 (s, 3H, OCH_3), 3.28 (dd, *J* = 5.6, 17.9 Hz, 1H, one proton of pyrazoline-CH_2); MS (m/z (R.I. %)): $[M]^+$ 424 (35.3), 290 (80.4), 272 (100), 170 (30), 115 (44.2); Anal. Calcd. for $C_{26}H_{21}FN_4O$ (424.17); % C, 73.57; H, 4.99; N, 13.20, Found: % C, 73.49; H, 5.12; N, 13.13.

3.1.1.10. *3-(5-(3-fluorophenyl)-4,5-dihydro-3-(3-methoxyphenyl)pyrazol-1-yl)-6-phenylpyridazine (IXj)*

Yellowish powder (yield 55%); m.p. 177-179 ^oC; IR ($\upsilon_{max.}/cm^{-1}$) 3082 (C-H aromatic), 1649 (C=N) and at 1593 (C=C); ^{1}HNMR (400 MHz, DMSO-d_6) δ *ppm*: 8.08 (d, *J* = 9.5 Hz, 1H, Ar-H), 8.01 (d, *J* = 7.6 Hz, 2H, Ar-H), 7.86 (d, *J* = 9.3 Hz, 1H, Ar-H), 7.36-7.51 (m, 7H, Ar-H), 7.01-7.16 (m, 4H, Ar-H), 5.94 (dd, *J* = 5.5, 12.1 Hz, 1H, pyrazoline-CH), 4.01 (dd, *J* = 12.2, 17.9 Hz, 1H, one proton of pyrazoline-CH_2), 3.83 (s, 3H, OCH_3), 3.30 (dd, *J* = 5.6, 17.9 Hz, 1H, one proton of pyrazoline-CH_2); ^{13}CNMR (100 MHz, DMSO-d_6) δ *ppm*: 161.6, 159.9, 155.9, 152.6, 152.3, 146.1, 136.8, 133.2, 131.2, 130.4, 129.3, 126.2, 122.2, 119.4, 116.3, 115.4, 114.5, 114.3, 113.3, 111.7, 61.8, 55.7, 43.1; MS (m/z (R.I. %)): $[M]^+$ 424 (21.9), 290 (100), 170 (16.2), 115 (33.7); Anal. Calcd. for $C_{26}H_{21}FN_4O$ (424.17); % C, 73.57; H, 4.99; N, 13.20, Found: % C, 73.62; H, 4.94; N, 13.29.

3.1.1.11. 3-(5-(4-fluorophenyl)-4,5-dihydro-3-(3-methoxyphenyl)pyrazol-1-yl)-6-phenylpyridazine (IXk).

White powder (yield 63%); m.p. 185-187 ^{o}C; IR ($\upsilon_{max.}$/cm^{-1}) 3056 (C-H aromatic), 1649 (C=N) and at 1598 (C=C); ^{1}HNMR (400 MHz, DMSO-d$_6$) δ *ppm*: 8.06 (d, *J* = 9.3 Hz, 1H, Ar-H), 7.99 (d, *J* = 7.6 Hz, 2H, Ar-H), 7.83 (d, *J* = 9.3 Hz, 1H, Ar-H), 7.68 (d, *J* = 7.6 Hz, 2H, Ar-H),7.33-7.45 (m, 5H, Ar-H), 7.21-7.26 (m, 2H, Ar-H),7.03-7.09 (m, 2H, Ar-H), 5.92 (dd, *J* = 5.5, 12.2 Hz, 1H, pyrazoline-CH), 3.98 (dd, *J* = 12.2, 17.9 Hz, 1H, one proton of pyrazoline-CH$_2$), 3.82 (s, 3H, OCH$_3$), 3.31 (dd, *J* = 5.5, 17.9 Hz, 1H, one proton of pyrazoline-CH$_2$); MS (m/z (R.I. %)): [M]$^{+}$ 424 (2), 421 (23.1), 135 (56.1), 57 (100); Anal. Calcd. for $C_{26}H_{21}FN_4O$ (424.17); % C, 73.57; H, 4.99; N, 13.20, Found: % C, 73.65; H, 4.89; N, 13.31.

3.1.1.12. 3-(4,5-dihydro-3-(3-methoxyphenyl)-5-m-tolylpyrazol-1-yl)-6-phenyl-pyridazine (IXl).

Yellow powder (yield 66%); m.p. 195-197 ^{o}C; IR ($\upsilon_{max.}$/cm^{-1}) 3057 (C-H aromatic), 1647 (C=N) and at 1598 (C=C); ^{1}HNMR (400 MHz, DMSO-d$_6$) δ *ppm*: 8.06 (d, *J* = 8.8 Hz, 1H, Ar-H), 7.97-8.01 (m, 2H, Ar-H), 7.84 (d, *J* = 9.3 Hz, 1H, Ar-H), 7.33-7.49 (m, 6H, Ar-H), 6.97-7.10 (m, 5H, Ar-H), 5.92 (dd, *J* = 5.5, 12.1 Hz, 1H, pyrazoline-CH), 3.98 (dd, *J* = 12.2, 17.8 Hz, 1H, one proton of pyrazoline-CH$_2$), 3.82 (s, 3H, OCH$_3$), 3.28 (dd, *J* = 5.6, 17.8 Hz, 1H, one proton of pyrazoline-CH$_2$), 2.26 (s, 3H, CH$_3$); ^{13}CNMR (100 MHz, DMSO-d$_6$) δ *ppm*: 164.4, 159.1, 155.0, 152.7, 144.7, 136.4, 130.2, 129.9, 129.4, 128.6, 128.3, 128.0, 127.6, 126.7, 126.1, 122.0, 121.8, 118.2, 116.8, 115.3, 114.5, 63.3, 55.3, 46.7, 21.5; MS (m/z (R.I. %)): [M]$^{+}$ 420 (5.4), 135 (78.1), 57 (100); Anal. Calcd. for $C_{27}H_{24}N_4O$ (420.20); % C, 77.12; H, 5.75; N, 13.32, Found: % C, 77.17; H, 5.69; N, 13.21.

3.1.1.13. 3-(5-(4-chlorophenyl)-4,5-dihydro-3-(3-methoxyphenyl)pyrazol-1-yl)-6-phenylpyridazine (IXm).

Buff powder (yield 67%); m.p. 144-146 ^{o}C; IR ($\upsilon_{max.}$/cm^{-1}) 3036 (C-H aromatic), 1695 1649 (C=N) and at 1592 (C=C); ^{1}HNMR (400 MHz, DMSO-d$_6$) δ *ppm*: 8.07 (d, *J* = 9.3 Hz, 1H, Ar-H), 8.00 (d, *J* = 7.3 Hz, 2H, Ar-H), 7.85 (d, *J* = 9.5 Hz, 1H, Ar-H), 7.45-7.51 (m, 2H, Ar-H), 7.37-7.44 (m, 6H, Ar-H), 7.30-7.34 (m, 2H, Ar-H), 7.03 (d, *J* = 6.9 Hz, 1H, Ar-H), 5.93 (dd, *J* = 5.5, 12.10 Hz, 1H, pyrazoline-CH), 4.01 (dd, *J* =

12.1, 17.7 Hz, 1H, one proton of pyrazoline-CH_2), 3.83 (s, 3H, OCH_3), 3.28 (dd, *J* = 5.5, 18.0 Hz, 1H, one proton of pyrazoline-CH_2); ^{13}CNMR (100 MHz, DMSO-d_6) *δ ppm*: 159.9, 155.8, 152.6, 152.2, 142.1, 136.8, 133.2, 132.1, 130.4, 129.3, 129.2, 128.2, 127.5, 126.2, 119.4, 116.3, 115.3, 111.7, 61.6, 55.7, 43.0; MS (m/z (R.I. %)): $[M]^+$ 440 (25.8), $[M+2]^+$ 442 (9.5), 306 (100), 308 (36.9); Anal. Calcd. for $C_{26}H_{21}ClN_4O$ (440.14); % C, 70.82; H, 4.80; N, 12.71, Found: % C, 70.73; H, 4.89; N, 12.65.

3.1.1.14. *3-(5-(4-fluoro-3-methoxyphenyl)-4,5-dihydro-3-(3-methoxyphenyl)-pyrazol-1-yl)-6-phenylpyridazine (IXn)*

Yellow powder (yield 61%); m.p. 175-177 ^oC; IR ($\upsilon_{max.}$/cm^{-1}) 3056 (C-H aromatic), 1650 (C=N) and at 1598 (C=C); ^{1}HNMR (400 MHz, DMSO-d_6) *δ ppm*: 8.07 (d, *J* = 9.3 Hz, 1H, Ar-H), 8.00 (d, *J* = 7.3 Hz, 2H, Ar-H), 7.86 (d, *J* = 9.5 Hz, 1H, Ar-H), 7.34-7.53 (m, 6H, Ar-H), 7.07-7.20 (m, 2H, Ar-H), 7.03 (d, *J* = 6.6 Hz, 1H, Ar-H), 6.76 (br. s, 1H, Ar-H), 5.91 (dd, *J* = 5.5, 11.9 Hz, 1H, pyrazoline-CH), 4.00 (dd, *J* = 12.2, 17.9 Hz, 1H, one proton of pyrazoline-CH_2), 3.80-3.86 (m, 6H, 2-OCH_3), 3.29 (dd, *J* = 5.5, 17.9 Hz, 1H, one proton of pyrazoline-CH_2); ^{13}CNMR (101 MHz, DMSO-d_6) *δ ppm*: 159.9, 156.0, 152.6, 152.2, 149.8, 147.7, 139.9, 136.8, 133.3, 130.3, 129.3, 126.2, 126.1, 119.3, 117.9, 117.8, 116.5, 116.2, 115.4, 112.0, 111.7, 61.9, 56.4, 55.7, 43.2; MS (m/z (R.I. %)): $[M]^+$ 454 (25.8), 320 (100), 170 (13.5), 115 (25.5); Anal. Calcd. for $C_{27}H_{23}FN_4O_2$ (454.18); % C, 71.35; H, 5.10; N, 12.33, Found: % C, 71.42; H, 4.98; N, 12.41.

3.2. In vitro cytotoxicity

In vitro cytotoxicity is made according to reported method[62]. The detailed procedures were supplied in Supplementary data.

3.3. EGFR inhibition assay:

HTRF (homogeneous time-resolved fluorescence) assay method was used to conduct inhibitory action of all newly synthesized compounds against EGFR [63]. EGFR kinase (BioAssay Systems - Kinase Assay Kit (EKIN-400)–(CA 94545, USA) and its substrate were incubated for 5 min in a buffer solution with newly synthesized compounds/Erlotinib to initiate the enzymatic reaction, then ATP was added to the reaction mixture. Hold under 30 min at room temperature. The reaction was stopped by

adding detection reagents containing EDTA for 1 h then the IC_{50} values have been determined.

3.4. Cell cycle analysis

UO-31 cells were seeded for 24 h at density of 1 x 10^5 cells per well and into six well plates. Added fetal bovine serum (FBS, 10 percent), after cells incubated at 37 °C and 5 percent CO_2. The medium was replaced with (DMSO 0.1% v/v) containing the 10 μM of compounds IXn and IXg , then incubated for 48 h, washed with cold phosphate buffered saline (PBS), fixed with 70% ethanol, rinsed with PBS then stained with the DNA fuorochrome PI, kept for 15 min. at 37 °C. A FACS Caliber flow cytometer was then used to test samples [64].

3.5. Annexin V-FITC apoptosis assay

Cells were incubated with the tested compounds IXn and IXg for 24. Then, trypsinized and washed with cold phosphate-buffer saline (PBS), then stained with Annexin V-FITC and PI in binding buffer for 15 min. at room temperature in the dark. The samples were analyzed using the flow cytometer [65].

3.6. In vitro ElISA immunoassay for cell death modulators

The levels of anti-apoptotic marker Bcl2 as well as the apoptotic marker Bax were measured in UO-31cells treated with the molecules **IXg, IXn** and PG for 24 h using ELISA colorimetric kits. All the procedures were performed according to the manufacturer's instructions [66]. On the other hand, the activation of caspase 3 was measured using DRG Caspase-3 (human) ELISA (EIA-4860) kit (DRG International Inc., USA), according to the manufacturer instructions.

3.7. Molecular docking study

The crystal structures of EGFR domain co-crystallized with Erlotinib (PDB ID: 1M17) were retrieved from the RCSB Protein Data Bank [67, 68]. The bound water and ligands not active in binding have been eliminated from the protein and added polar hydrogen. Then, the protein was prepared in MOE with default options for docking study using Protonate 3D protocol. The entire EGFR complex had been defined as a docking receptor binding site. Docking was done using Triangle Matcher placement

method and London dG scoring function. The docking setup was initially validated by redocking the co-crystallized ligand (Erlotinib) in the vicinity of the enzyme binding site, then removing the Erlotinib molecule and inserting the target compound during the molecular docking process. Types of docked protein interactions with ligand were analyzed after molecular docking ended.

4. Conclusion

New series of pyridazine hybridized with pyrazoline derivatives were designed and synthesized based on targeting EGFR. Preliminarily screening results at NCI, USA showed the sensitivity of Ovarian cancer IGROV1, Breast cancer T-47D, Renal cancer CAKI-1 and UO-31 cell lines to almost all screened compounds. EGFR inhibition for the promising cytotoxic compounds showed that compounds **IXn**, **IXg**, **IXb** and **IXl** exhibited inhibition effect more than Erlotinib. Also, compounds **IXg** and **IXn** showed high cell accumulation at phase G2/M phase in UO-31cells confirming its arresting cell cycle at G2/M phase. Furthermore, compounds **IXg** and **IXn** elevated Bax/Bcl2 ratio and show a pronounced enhancement in the levels of the active caspases -3 which confirmed the mechanistic pathway of them. Molecular docking study of compounds **IXg** and **IXn** showed high degrees of superimposition Erlotinib into EGFR active sites. These results were in a perfect match with the EGFR enzyme inhibition assay.

Acknowledgement

The authors would like to extend their sincere appreciation to Taif University Researchers Supporting Project number (TURSP-2020/56), Taif University, Taif, Saudi Arabia. Authors are thankful to the Developmental Therapeutics Program of the United States, National Cancer Institute for performing the anticancer testing.

Supplementary data.

Supplementary materials associated with this research including NCI cytotoxicity results and elemental and spectroscopic analyses are available.

References

[1] A. Ayati, S. Emami, A. Asadipour, A. Shafiee, A. Foroumadi, Recent applications of 1,3-thiazole core structure in the identification of new lead compounds and drug discovery, Eur J Med Chem 97 (2015) 699-718.
[2] R.M. Aly, R.A.T. Serya, A.M. El-Motwally, A. Esmat, S. Abbas, D.A. Abou El Ella, Novel quinoline-3-carboxamides (Part 2): Design, optimization and synthesis of quinoline based scaffold as EGFR inhibitors with potent anticancer activity, Bioorg Chem 75 (2017) 368-392.
[3] G. Mountzios, Lung cancer: biology and technology foster therapeutic innovation, Ann Transl Med 6 (2018) 137.
[4] S. Bishayee, Role of conformational alteration in the epidermal growth factor receptor (EGFR) function, Biochem Pharmacol 60 (2000) 1217-23.
[5] H. Ogiso, R. Ishitani, O. Nureki, S. Fukai, M. Yamanaka, J.H. Kim, K. Saito, A. Sakamoto, M. Inoue, M. Shirouzu, S. Yokoyama, Crystal structure of the complex of human epidermal growth factor and receptor extracellular domains, Cell 110 (2002) 775-87.
[6] T. Holbro, G. Civenni, N.E. Hynes, The ErbB receptors and their role in cancer progression, Exp Cell Res 284 (2003) 99-110.
[7] N.E. Hynes, K. Horsch, M.A. Olayioye, A. Badache, The ErbB receptor tyrosine family as signal integrators, Endocr Relat Cancer 8 (2001) 151-9.
[8] J. Capdevila, E. Elez, T. Macarulla, F.J. Ramos, M. Ruiz-Echarri, J. Tabernero, Anti-epidermal growth factor receptor monoclonal antibodies in cancer treatment, Cancer Treat Rev 35 (2009) 354-63.
[9] D.A. Reardon, P.Y. Wen, I.K. Mellinghoff, Targeted molecular therapies against epidermal growth factor receptor: past experiences and challenges, Neuro Oncol 16 Suppl 8 (2014) viii7-13.
[10] P. Seshacharyulu, M.P. Ponnusamy, D. Haridas, M. Jain, A.K. Ganti, S.K. Batra, Targeting the EGFR signaling pathway in cancer therapy, Expert Opin Ther Targets 16 (2012) 15-31.
[11] T.K. Olszewski, B. Boduszek, Synthesis of new thiazole-2,-4, and-5-yl-(amino) methylphosphonates and phosphinates: unprecedented cleavage of thiazole-2 derivatives under acidic conditions., Tetrahedron 66 (2010) 8661-8666.
[12] T.D. Penning, J.J. Talley, S.R. Bertenshaw, J.S. Carter, P.W. Collins, S. Docter, M.J. Graneto, L.F. Lee, J.W. Malecha, J.M. Miyashiro, R.S. Rogers, D.J. Rogier, S.S. Yu, AndersonGd, E.G. Burton, J.N. Cogburn, S.A. Gregory, C.M. Koboldt, W.E. Perkins, K. Seibert, A.W. Veenhuizen, Y.Y. Zhang, P.C. Isakson, Synthesis and biological evaluation of the 1,5-diarylpyrazole class of cyclooxygenase-2 inhibitors: identification of 4-[5-(4-methylphenyl)-3-(trifluoromethyl)-1H-pyrazol-1-yl]benze nesulfonamide (SC-58635, celecoxib), J Med Chem 40 (1997) 1347-65.
[13] R. Sridhar, P.T. Perumal, S. Etti, G. Shanmugam, M.N. Ponnuswamy, V.R. Prabavathy, N. Mathivanan, Design, synthesis and anti-microbial activity of 1H-pyrazole carboxylates, Bioorg Med Chem Lett 14 (2004) 6035-40.
[14] G. Menozzi, L. Mosti, P. Fossa, F. Mattioli, M. Ghia, ω-Dialkylaminoalkyl ethers of phenyl-(5-substituted-1-phenyl-1H-pyrazol-4-yl)methanols with analgesic and anti-inflammatory activity., J. Heterocycl. Chem. 34 (1997) 963-968.
[15] H.A. Abdel-Aziz, A.A. Mekawey, K.M. Dawood, Convenient synthesis and antimicrobial evaluation of some novel 2-substituted-3-methylbenzofuran derivatives, Eur J Med Chem 44 (2009) 3637-44.

[16] H.A. Abdel-Aziz, H.S. El-Zahabi, K.M. Dawood, Microwave-assisted synthesis and in-vitro anti-tumor activity of 1,3,4-triaryl-5-N-arylpyrazole-carboxamides, Eur J Med Chem 45 (2010) 2427-32.
[17] F.M. Awadallah, G.A. Piazza, B.D. Gary, A.B. Keeton, J.C. Canzoneri, Synthesis of some dihydropyrimidine-based compounds bearing pyrazoline moiety and evaluation of their antiproliferative activity, Eur J Med Chem 70 (2013) 273-9.
[18] C.N. Cavasotto, M.A. Ortiz, R.A. Abagyan, F.J. Piedrafita, In silico identification of novel EGFR inhibitors with antiproliferative activity against cancer cells, Bioorg Med Chem Lett 16 (2006) 1969-74.
[19] Y.R. Liu, J.Z. Luo, P.P. Duan, J. Shao, B.X. Zhao, J.Y. Miao, Synthesis of pyrazole peptidomimetics and their inhibition against A549 lung cancer cells, Bioorg Med Chem Lett 22 (2012) 6882-7.
[20] P.C. Lv, D.D. Li, Q.S. Li, X. Lu, Z.P. Xiao, H.L. Zhu, Synthesis, molecular docking and evaluation of thiazolyl-pyrazoline derivatives as EGFR TK inhibitors and potential anticancer agents, Bioorg Med Chem Lett 21 (2011) 5374-7.
[21] I. Vujasinovic, A. Paravic-Radicevic, K. Mlinaric-Majerski, K. Brajsa, B. Bertosa, Synthesis and biological validation of novel pyrazole derivatives with anticancer activity guided by 3D-QSAR analysis, Bioorg Med Chem 20 (2012) 2101-10.
[22] H.S. Abbas, S.S. Abd El-Karim, Design, synthesis and anticervical cancer activity of new benzofuran-pyrazol-hydrazono- thiazolidin-4-one hybrids as potential EGFR inhibitors and apoptosis inducing agents, Bioorg Chem 89 (2019) 103035.
[23] K.M. Qiu, H.H. Wang, L.M. Wang, Y. Luo, X.H. Yang, X.M. Wang, H.L. Zhu, Design, synthesis and biological evaluation of pyrazolyl-thiazolinone derivatives as potential EGFR and HER-2 kinase inhibitors, Bioorg Med Chem 20 (2012) 2010-8.
[24] X.X. Tao, Y.T. Duan, L.W. Chen, D.J. Tang, M.R. Yang, P.F. Wang, C. Xu, H.L. Zhu, Design, synthesis and biological evaluation of pyrazolyl-nitroimidazole derivatives as potential EGFR/HER-2 kinase inhibitors, Bioorg Med Chem Lett 26 (2016) 677-683.
[25] H.H. Wang, K.M. Qiu, H.E. Cui, Y.S. Yang, L. Yin, M. Xing, X.Y. Qiu, L.F. Bai, H.L. Zhu, Synthesis, molecular docking and evaluation of thiazolyl-pyrazoline derivatives containing benzodioxole as potential anticancer agents, Bioorg Med Chem 21 (2013) 448-55.
[26] W.M. Zhang, M. Xing, T.T. Zhao, Y.J. Ren, X.H. Yang, Y.S. Yang, P.C. Lv, H.L. Zhu, Synthesis, molecular modeling and biological evaluation of cinnamic acid derivatives with pyrazole moieties as novel anticancer agents., RSC advances 4 (2014) 37197-37207.
[27] M.V. Reddy, C.R. Su, W.F. Chiou, Y.N. Liu, R.Y. Chen, K.F. Bastow, K.H. Lee, T.S. Wu, Design, synthesis, and biological evaluation of Mannich bases of heterocyclic chalcone analogs as cytotoxic agents, Bioorg Med Chem 16 (2008) 7358-7370.
[28] J.V. Faria, P.F. Vegi, A.G.C. Miguita, M.S. Dos Santos, N. Boechat, A.M.R. Bernardino, Recently reported biological activities of pyrazole compounds, Bioorg Med Chem 25 (2017) 5891-5903.
[29] B. Insuasty, A. Tigreros, F. Orozco, J. Quiroga, R. Abonia, M. Nogueras, A. Sanchez, J. Cobo, Synthesis of novel pyrazolic analogues of chalcones and their 3-aryl-4-(3-aryl-4,5-dihydro-1H-pyrazol-5-yl)-1-phenyl-1H-pyrazole derivatives as potential antitumor agents, Bioorg Med Chem 18 (2010) 4965-74.

[30] M. Labbozzetta, R. Baruchello, P. Marchetti, M.C. Gueli, P. Poma, M. Notarbartolo, D. Simoni, N. D'Alessandro, Lack of nucleophilic addition in the isoxazole and pyrazole diketone modified analogs of curcumin; implications for their antitumor and chemosensitizing activities, Chem Biol Interact 181 (2009) 29-36.

[31] M. Asif, The biological potentials of substituted 1, 2-diazines: a review on versatile pyridazine derivatives., Journal of Chinese Pharmaceutical Sciences 25 (2016) 707-725.

[32] M. Asif, A Review on Pyridazinone Ring Containing Various Cardioactive Agents., Journal of Chemical Reviews 1 (2019) 66-77.

[33] M.J. Kim, J. Lee, S.Y. Kang, S.H. Lee, E.J. Son, M.E. Jung, K.S. Song, M. Lee, H.K. Han, J. Kim, Novel C-aryl glucoside SGLT2 inhibitors as potential antidiabetic agents: Pyridazinylmethylphenyl glucoside congeners, Bioorg Med Chem Lett 20 (2010) 3420-5.

[34] H.M. Faidallah, K.A. Khan, M.S. Makki, Synthesis and Biological Evaluation of New Fused Isoxazolo [4, 5-d] Pyridazine Derivatives., Journal of the Chinese Chemical Society 58 (2011) 191-198.

[35] A.A. Siddiqui, R. Mishra, M. Shaharyar, Synthesis, characterization and antihypertensive activity of pyridazinone derivatives, Eur J Med Chem 45 (2010) 2283-90.

[36] S. Ahmad, I.G. Rathish, S. Bano, M.S. Alam, K. Javed, Synthesis and biological evaluation of some novel 6-aryl-2-(p-sulfamylphenyl)-4,5-dihydropyridazin-3(2H)-ones as anti-cancer, antimicrobial, and anti-inflammatory agents, J Enzyme Inhib Med Chem 25 (2010) 266-71.

[37] N.A. El-Ghaffar, M.K. Mohamed, M.S. Kadah, A.M. Radwan, G.H. Said, S.N. Abd, Synthesis and anti-tumor activities of some new pyridazinones containing the 2-phenyl-1H-indolyl moiety., Journal of Chemical and Pharmaceutical Research 3 (2011) 248-259.

[38] E.F. Ewies, M.F. El-Shehry, L.S. Boulos, Synthesis of some novel pyridazine derivatives of expected antitumor activity, Int. J. Chem. Tech. Res. 7 (2015) 2506–2513.

[39] E. Lattmann, W.O. Ayuko, D. Kinchinaton, C.A. Langley, H. Singh, L. Karimi, M.J. Tisdale, Synthesis and evaluation of 5-arylated 2(5H)-furanones and 2-arylated pyridazin-3(2H)-ones as anti-cancer agents, J Pharm Pharmacol 55 (2003) 1259-65.

[40] M.S.R. Murty, B.R. Rao, K.R. Ram, J.S. Yadav, J. Antony, R.J. Anto, Synthesis and preliminary evaluation activity studies of novel 4-(aryl/heteroaryl-2-ylmethyl)-6-phenyl-2-[3-(4-substituted-piperazine-1-yl) propyl] pyridazin-3 (2H)-one derivatives as anticancer agents., Medicinal chemistry research 21 (2012) 3161-3169.

[41] M.F. Brana, M. Cacho, M.L. Garcia, E.P. Mayoral, B. Lopez, B. de Pascual-Teresa, A. Ramos, N. Acero, F. Llinares, D. Munoz-Mingarro, O. Lozach, L. Meijer, Pyrazolo[3,4-c]pyridazines as novel and selective inhibitors of cyclin-dependent kinases, J Med Chem 48 (2005) 6843-54.

[42] H. Djaballah, H.E. Varmus, D. Shum, R. Somwar, A. Chucholowski, M.S. Thiruvazhi, Substituted pyridazines as EGFR and/or KRAS inhibitors, U.S. Patent (2017) 9,562,019.

[43] M. Decker, Hybrid molecules incorporating natural products: applications in cancer therapy, neurodegenerative disorders and beyond, Curr Med Chem 18 (2011) 1464-75.
[44] Y.C. Duan, Y.C. Zheng, X.C. Li, M.M. Wang, X.W. Ye, Y.Y. Guan, G.Z. Liu, J.X. Zheng, H.M. Liu, Design, synthesis and antiproliferative activity studies of novel 1,2,3-triazole-dithiocarbamate-urea hybrids, Eur J Med Chem 64 (2013) 99-110.
[45] Y.C. Mayur, G.J. Peters, V.V. Prasad, C. Lemo, N.K. Sathish, Design of new drug molecules to be used in reversing multidrug resistance in cancer cells, Curr Cancer Drug Targets 9 (2009) 298-306.
[46] W.J. Coates, A. McKillop, One-pot preparation of 6-substituted 3 (2H)-pyridazinones from ketones. Synthesis, Synthesis 3 (1993) 334-342.
[47] A.E. Kummerle, M.M. Vieira, M. Schmitt, A.L. Miranda, C.A. Fraga, J.J. Bourguignon, E.J. Barreiro, Design, synthesis and analgesic properties of novel conformationally-restricted N-acylhydrazones (NAH), Bioorg Med Chem Lett 19 (2009) 4963-6.
[48] R.F. George, M. Kandeel, D.Y. El-Ansary, A.M. El Kerdawy, Some 1,3,5-trisubstituted pyrazoline derivatives targeting breast cancer: Design, synthesis, cytotoxic activity, EGFR inhibition and molecular docking, Bioorg. Chem. 99 (2020) 103780.
[49] G. Wang, W. Liu, Z. Gong, Y. Huang, Y. Li, Z. Peng, Synthesis, biological evaluation, and molecular modelling of new naphthalene-chalcone derivatives as potential anticancer agents on MCF-7 breast cancer cells by targeting tubulin colchicine binding site, J Enzyme Inhib Med Chem 35 (2020) 139-144.
[50] T. Bakó, P. Bakó, G. Keglevich, P. Bombicz, M. Kubinyi, K. Pál, S. Bodor, A. Makó, L. Tőke, Phase-transfer catalyzed asymmetric epoxidation of chalcones using chiral crown ethers derived from D-glucose, D-galactose, and D-mannitol., Tetrahedron: Asymmetry 15 (2004) 1589-1595.
[51] M.C. Cardia, M.L. Sanna, R. Meleddu, S. Distinto, M. Yañez, D. Viña, M. Lamela, E. Maccioni, A Novel Series of 3, 4-Disubstituted Dihydropyrazoles: Synthesis and Evaluation for MAO Enzyme Inhibition., Journal of Heterocyclic Chemistry 50 (2013) E87-E92.
[52] L.D. Hicks, A.J. Fry, V.C. Kurzweil, Ab initio computation of electron affinities of substituted benzalacetophenones (chalcones): a new approach to substituent effects in organic electrochemistry., Electrochimica acta 50 (2004) 1039-1047.
[53] J. Ju, L. Zhang, R. Hua, Palladium-catalyzed direct intramolecular double α-C–H arylation of 1, 5-diketone: a strategy for synthesis of Tröger's base analogues., Tetrahedron Letters 55 (2014) 3374-3376.
[54] A. Link, C. Kunick, d-Fused [1]benzazepines with selective in vitro antitumor activity: synthesis and structure-activity relationships, J Med Chem 41 (1998) 1299-305.
[55] P.C. Lv, J. Sun, Y. Luo, Y. Yang, H.L. Zhu, Design, synthesis, and structure-activity relationships of pyrazole derivatives as potential FabH inhibitors, Bioorg Med Chem Lett 20 (2010) 4657-60.
[56] P.M. Sivakumar, S. Ganesan, P. Veluchamy, M. Doble, Novel chalcones and 1, 3, 5-triphenyl-2-pyrazoline derivatives as antibacterial agents., Chemical biology & drug design 76 (2010) 407-411.
[57] Y. Weng, Q. Chen, W. Su, Copper-catalyzed intramolecular tandem reaction of (2-halogenphenyl)(3-phenyloxiran-2-yl)methanones: synthesis of (Z)-aurones, J Org Chem 79 (2014) 4218-24.

[58] I. Dolka, M. Krol, R. Sapierzynski, Evaluation of apoptosis-associated protein (Bcl-2, Bax, cleaved caspase-3 and p53) expression in canine mammary tumors: An immunohistochemical and prognostic study, Res Vet Sci 105 (2016) 124-33.
[59] J.M. Golbano, P. Loppez-Aparicio, M.N. Recio, M.A. Perez-Albarsanz, Finasteride induces apoptosis via Bcl-2, Bcl-xL, Bax and caspase-3 proteins in LNCaP human prostate cancer cell line, Int J Oncol 32 (2008) 919-24.
[60] D.G. Tang, A.T. Porter, Target to apoptosis: a hopeful weapon for prostate cancer, Prostate 32 (1997) 284-93.
[61] X.Y. Meng, H.X. Zhang, M. Mezei, M. Cui, Molecular docking: a powerful approach for structure-based drug discovery, Curr Comput Aided Drug Des 7 (2011) 146-57.
[62] A. Monks, D. Scudiero, P. Skehan, R. Shoemaker, K. Paull, D. Vistica, C. Hose, J. Langley, P. Cronise, A. Vaigro-Wolff, et al., Feasibility of a high-flux anticancer drug screen using a diverse panel of cultured human tumor cell lines, J Natl Cancer Inst 83 (1991) 757-66.
[63] Y. Jia, C.M. Quinn, A.I. Gagnon, R. Talanian, Homogeneous time-resolved fluorescence and its applications for kinase assays in drug discovery, Anal. Biochem. 356 (2006) 273-281.
[64] J. Wang, M.J. Lenardo, Roles of caspases in apoptosis, development, and cytokine maturation revealed by homozygous gene deficiencies, J Cell Sci 113 (Pt 5) (2000) 753-7.
[65] K.K. Lo, T.K. Lee, J.S. Lau, W.L. Poon, S.H. Cheng, Luminescent biological probes derived from ruthenium(II) estradiol polypyridine complexes, Inorg Chem 47 (2008) 200-8.
[66] E.F. Abdelhaleem, M.K. Abdelhameid, A.E. Kassab, M.M. Kandeel, Design and synthesis of thienopyrimidine urea derivatives with potential cytotoxic and pro-apoptotic activity against breast cancer cell line MCF-7, Eur J Med Chem 143 (2018) 1807-1825.
[67] http://www.rcsb.org/.
[68] J. Stamos, M.X. Sliwkowski, C. Eigenbrot, Structure of the epidermal growth factor receptor kinase domain alone and in complex with a 4-anilinoquinazoline inhibitor, J Biol Chem 277 (2002) 46265-72.

Declaration of Competing Interest:

The authors declare no conflict of interest.